Modern Pathology (2010) 23, 1567–1576

Biologic profiling of lymph node negative breast cancers by means of microRNA expression

Emiel AM Janssen[1], Aida Slewa[1], Einar Gudlaugsson[1,2], Kristin Jonsdottir[1,2], Ivar Skaland[1], Håvard Søiland[3] and Jan PA Baak[1,2,4]

[1]*Department of Pathology, Stavanger University Hospital, Stavanger, Norway;* [2]*The Gade Institute, University of Bergen, Bergen, Norway;* [3]*Department of Surgery, Stavanger University Hospital, Stavanger, Norway and* [4]*Free University, Amsterdam, The Netherlands*

Breast cancer is a heterogeneous disease. Different subgroups can be recognized on the basis of the steroid receptors, HER-2, cytokeratin expression and proliferation patterns. As a result of mRNA-profiling studies, five major groups can be recognized, of which the triple-negative and basal-like tumors have the worst prognosis. Many of these tumors have a high proliferation that has the strongest prognostic value in node negative breast cancer. In the current study we analyzed the microRNA pattern in 103 lymph node negative breast cancers and compared these profiles with different biological characteristics and clinicopathological features. Unsupervised hierarchical cluster analysis divides the patients into four main groups, of which the basal-like/triple-negative group is the most prominent (11% of all cases), the luminal A cancers containing the Her2 negative and estrogen receptor/progesterone receptor-positive tumors is the largest group (57%), and the group of luminal B (32%) is more heterogeneous and contains the Her2 positive/estrogen receptor-negative patients as well. The highest overall classification values by analysis of variance followed by cross validation (leave one sample out and reselect genes) were found for cytokeratin 5 and 6, triple-negative and estrogen receptor, with 97, 90 and 90% accuracy, respectively. *MiR-106b* gene is prominent in all of these signatures and correlates strongest with high proliferation. Other interesting observations are the presence of several microRNAs (*miR532-5p*, *miR-500*, *miR362-5p*, and *miR502-3p*) located at Xp11.23 in cancers with a triple-negative signature, and the upregulation of several *miR-17* cluster members in estrogen receptor-negative tumors. The current study shows that estrogen receptor negativity and cytokeratin 5 and 6 expression are important, and specific biological processes in lymph node negative breast cancer, as microRNA signatures are strongest in these subgroups.
Modern Pathology (2010) **23,** 1567–1576; doi:10.1038/modpathol.2010.177; published online 3 September 2010

Keywords: breast; cancer; microRNA; profiling

Since the publication of the human genome and the development of high-throughput array-based gene expression profiling platforms, knowledge about breast cancer and its genetic background has increased enormously. On the basis of the gene expression, invasive breast cancers can be classified into three major subtypes: luminal, basal-like and Her2/neu-overexpressing.[1] Many investigators have used surrogate immunohistochemical markers to classify these tumors: estrogen receptor, progesterone receptor, and HER2 negative breast cancers (=triple-negative breast cancer profile) are classified as normal breast-like if basal cytokeratins and epidermal growth factor receptor are lacking, and basal-cell-like cancers when basal cytokeratins (cytokeratin 5 and 6 and/or cytokeratin 14) are expressed.[2] Most breast cancer series contain 8–15% triple-negative tumors and 10–15% basal-like tumors. Triple-negative and basal-like breast cancers are often (but not always) associated with high proliferation, high grade, young age, BRCA1 and aggressive clinical behavior (30–50% mortality in lymph node negative cancers).[3] Furthermore, certain gene profiles correlate with estrogen receptor

Correspondence: Dr JPA Baak, Department of Pathology, Stavanger University Hospital, Box 8100, Stavanger 4068, Norway.
E-mail: jpabaak@yahoo.com
Received 1 July 2010; revised 23 July 2010; accepted 28 July 2010; published online 3 September 2010

expression, therapy response and resistance and survival outcome. Some of these gene profiles are currently being validated in large prospective multinational studies.

It is interesting that the gene signatures correlating with outcome contain high numbers of genes correlated to proliferation. A recent study even found that a signature based upon cell-cycle-related genes only, was a more accurate predictor of breast cancer clinical outcome than another FDA approved signature containing other genes as well.[4] Others[5] found that the simplest model defining the risk score as the expression of a single proliferation gene, yielded similar or even better performance than models fitted from genome-wide data, and also outperformed classical factors, such as histological grade. This is in agreement with previous retrospective and prospective studies performed on large numbers of lymph node negative breast cancer patients showing that proliferation measured by thymidine labeling index, mitotic activity index, or phosphohistone H3 are stronger prognosticators than classical predictors.[6] Moreover, in two independent studies, adjuvant chemotherapy was significantly beneficial for patients with rapidly proliferating tumors, but not for patients with slowly proliferating tumors.[7,8] A comparison between phosphohistone H3/mitotic activity index and gene signatures, however, has not yet been performed.

Recently an extra level of gene regulation was discovered: small non-coding RNA molecules called microRNAs. They have an important role in gene silencing by binding directly and specifically to mRNA molecules and enabling their degradation. The microRNAs are 19–25 nucleotides in length and compose the largest family of non-coding RNA's involved in gene silencing. Their functions are exerted through translational inhibition of the targeted mRNA by binding to the 3′-untranslated region (imperfect match) and degradation of target mRNA (perfect match).[9] The microRNAs are downregulated in a number of different tumors,[8,10] and in some cases the re-introduction of these microRNAs has been shown to impair the viability of cancer cells.[11]

In the current study, we investigated in microRNA arrays the correlation between microRNA expression and several important biological and prognostic breast cancer features, such as proliferation, estrogen receptor/progesterone receptor/Her2/cytokeratin 5 and 6 expression to better understand the fundamentals of the regulation of these features.

Materials and methods

Patients

The study was approved by the Regional Ethics Committee, the Norwegian Social Science Data Service, and the Norwegian Data Inspectorate. According to national guidelines from the Norwegian Breast Cancer Group, during the period 1993–1997, fresh frozen tumor tissue from each breast tumor patient was stored at the Department of Pathology of the Stavanger University Hospital for hormone receptor determination. In total, material from 235 individual patients was stored, of which 135 were lymph node negative. The following patients had to be excluded because of either bilateral disease ($n=3$), breast tumors in earlier years ($n=8$), lack of follow-up ($n=3$), lack of adequate material ($n=10$) or too poor quality RNA ($n=8$). This left 103 patients with adequate material and follow-up. Although these cases were selected on the basis of the presence of fresh frozen tissue, the distribution over the different classes was similar to the overall distribution in population-based studies in the province of Rogaland-South, Norway.[6] All patients had been treated with either modified radical mastectomy, or breast-conserving therapy with postoperative radiation. Additional adjuvant treatment, including peri-operative chemotherapy, postoperative radiation (also in selected patients treated with modified radical mastectomy) and endocrine adjuvant treatment (ie tamoxifen) was offered according to the national guidelines of the Norwegian Breast Cancer Group at the time of diagnosis.

Histopathology

The post-surgical size of the tumor was measured in fresh specimens; the tumors were sliced (0.5 cm), fixed in buffered 4% formaldehyde, and embedded in paraffin. Paraffin sections (4 μm) were stained with haematoxylin, eosin, and saffran. Histological type was assessed according to World Health Organization criteria.[12] Grade was assessed according to the Nottingham modification[13] on the basis of the careful examination by two pathologists with considerable experience in breast pathology, using the criteria mitotic activity index 0–5 = 1, mitotic activity index 6–10 = 2, and mitotic activity index >10 = 3; nuclear atypia mild = 1, moderate = 2, and marked = 3; and tubular formation majority (ie, >75%) = 1, moderate (10–75%) = 2, and little or none (<10%) = 3. Grade was the sum of mitotic activity index, nuclear atypia, and tubular formation values. Thus, a sum of 3–5 was Grade I, 6–7 was Grade II, and 8–9 was Grade III. Mitotic activity index was assessed as previously described.[14] Briefly, all unambiguous mitoses were counted with a conventional transmission light microscope with a $\times 40$ objective (450 μm at specimen level) in 10 consecutive neighboring fields of vision in the invasive, most cell-dense area in the periphery of the tumor (representing a total area of 1.59 mm^2 at the specimen level).

Immunohistochemistry

Antibody dilution and immunohistochemistry protocols were optimized before the study onset. To ensure uniform handling of samples, all sections

were processed simultaneously. Paraffin sections adjacent to the haematoxylin, eosin and saffran sections used for assessment of the mitotic activity index and histology were mounted onto Superfrost Plus slides (Menzel, Braunschweig, Germany) and dried overnight at 37°C followed by 1 h at 60°C. Sections were deparaffinized in xylene and rehydrated in decreasing concentrations of alcohol. Antigen was retrieved with a highly stabilized retrieval system (ImmunoPrep, Instrumec, Oslo, Norway) using 10 mM TRIS/1 mM EDTA (pH 9.0) as the retrieval buffer. Sections were heated for 3 min at 110°C followed by 10 min at 95°C and cooled to 20°C. Rabbit polyclonal anti-phosphohistone H3 (ser 10) (Upstate 06-570; Lake Placid, NY, USA) was used at a dilution of 1:1500. Cytokeratin 5 and 6 (Clone D5/16 B4, Dako, Glostrup, Denmark) was used at a dilution of 1/100. Estrogen receptor (clone SP1, Neomarkers/LabVision, Fremont, CA, USA) was used at a dilution 1/400. Progesterone receptor (Clone SP2, Neomarkers/LabVision) was used at a dilution of 1/1000. Anti-phosphohistone H3 was incubated for 60 min at 22°C. All the other antibodies were incubated for 30 min at 22°C Dako antibody diluent (S0809) was used. Endogenous peroxidase activity was blocked with a peroxidase-blocking reagent (S2001; Dako) for 10 min. The immune complex was visualized with the Dako REAL EnVision Detection System, Peroxidase/DAB, Rabbit/Mouse (K5007; Dako). Sections were incubated with EnVision/HRP, Rabbit/Mouse for 30 min and diaminobenzidine chromogen for 10 min. The sections were counterstained with haematoxylin, dehydrated, and mounted. All steps were performed using a Dako autostainer and TBS (S1968; Dako) with 0.05% Tween 20 as wash buffer. For HER2 assessments, Dako Herceptest was used according to the manufacturer's procedures.

Quantification of Immunohistochemical Stainings

The phosphohistone H3 index was assessed using the same counting protocol as for the mitotic activity index.[15] Two independent pathologists counted the number of phosphohistone H3-positive objects (nuclei and mitoses) in 10 adjacent fields of vision, with a $\times 40$ objective, as described above for mitoses. Nuclei with fine granular phosphohistone H3 staining were not counted, as these cells are not in the G2 phase.[16] Phosphohistone H3-rich areas are usually localized in the periphery (ie, growing zone) of the cancers. If the counts of two observers differed by more than three figures, the count was repeated with a multi-head microscope and a consensus score was obtained. In addition to performing subjective counts, phosphohistone H3 expression was evaluated using the fully automated Visiopharm Integrator System (VIS) analysis system (Visiopharm, Hørsholm, Denmark), following the same image processing principles described before.[6] Reproducibility of the phosphohistone H3 measurements between subjective counts by two observers, and between subjective and digital image analysis results was high ($R = 0.94$–0.98). Not surprisingly, the reproducibility of the phosphohistone H3 counts by the automated digital image analysis on different days by different observers was close to perfect ($R = 0.99$). For this reason, in the statistical analysis the image analysis counts were used.

The percentage of cytokeratin 5 and 6 positive tumor cells in each cancer was scored using a continuous scale of 0–100%. Estrogen receptor and progesterone receptor were scored as positive when nuclear staining was present in >10% of the tumor cells. HER2 was scored according to the Dako Hercep Test scoring protocol. All 2+ and 3+ cases were regarded as positive. All sections were independently scored by two pathologists.

RNA isolation/Labeling/Hybridization

At least two 10 μm cryosections were cut; to assess the number of tumor cells in the tissue all sections were evaluated by an experienced breast pathologist. Where possible, only material from the tumor area was isolated by means of macrodissection. All tissues contained at least 50% tumor cells. The RNA isolation method was chosen after careful comparison of different RNA isolation procedures. The MirVANA total RNA isolation kit (Ambion/Applied Biosystems, Austin, TX, USA) appeared to be the best-suited isolation method for use with Exiqon LNA microRNA profiling (unpublished results). Total RNA was isolated according to the protocol provided by the manufacturers. For quality control, all ($n = 109$) samples were analyzed by both Agilent Bioanalyzer 2100 (RNA and microRNA chips) and RNA measurement on the Nanodrop instrument. The samples were labeled using the miRCURY Hy3/Hy5 power labeling kit and hybridized on the miRCURY LNA Array (v.11.0, Exiqon A/S, Vedbaek, Denmark). These arrays contain melting temperature (Tm)-normalized capture probes for 2090 microRNA's (all human and viral microRNA's ($n = 838$) annotated in miRBase 11, as well as 427 proprietary microRNAs not yet included in miRBase 11.0), including the corresponding pre-microRNAs. The samples were hybridized on a hybridization station, where analysis of the scanned slides showed that the labeling was successful as all capture probes for the control spike-in oligonucleotides produced signals in the expected range. The quantified signals (background correction) were normalized using the global LOcally WEighted Scatterplot Smoothing (Lowess) regression algorithm, which produced the best within-slide normalization to minimize the intensity-dependent differences between the dyes. All hybridizations were made against a common reference pool consisting of all patient material combined.

microRNA Analysis

Data analysis was performed with only those microRNAs present in 10 or more samples ($n=604$). Using the free downloadable software package Dchip (version 31 March 2009; Dana-Farber Cancer Institute, Boston, MA, USA),[17] absolute correlations (including genes with opposite gene profiles) were calculated using analysis of variance with a *P*-value of ≤ 0.01. Gene lists created in this way were used to classify samples by linear discriminant analysis (LDA) and cluster analysis. Classification accuracy was tested by performing cross validation analysis (by leaving one sample out and reselecting genes). Gene lists and classification results were chosen according to the highest classification accuracy after cross validation.

Results

An overview of the clinicopathological features for all patients included in this study is given in Table 1. Unsupervised hierarchical cluster analysis divides the patients into four main groups (Figure 1), of which the basal-like/triple-negative group is the most prominent (11% of all cases), the luminal A cancers containing the Her2 negative and estrogen receptor/progesterone receptor-positive tumors is the largest group (57%), and the group of luminal B (32%) is more heterogeneous and contains the Her2 positive/estrogen receptor-negative patients as well. In the luminal B cancers, two smaller subgroups can be distinguished where only age is significantly different (67.6 *vs* 57.1), and although insignificant, there is also a trend towards higher proliferation in the older patient group (Table 2). analysis of variance *P*-values were lowest for cytokeratin 5 and 6 ($P=0.00000001$) and estrogen receptor ($P=0.0000001$). The microRNAs that correlated with the different clinicopathological features are listed in Table 3. It is interesting that *mir-106b*, *mir-29*, and their pre-microRNAs (*mir-106b** and *mir-29**) are present in several of the signatures. Hierarchical cluster analysis shows that the estrogen receptor-negative patients tend to overlap with the cytokeratin 5 and 6 positive patients, these patients are often under 55 years of age (median age = 49.5) and all have high proliferation (mitotic activity index ≥ 10 and phosphohistone H3 ≥ 13). The following microRNAs are positively correlated with proliferation (independent of which method (mitotic activity index or phosphohistone H3) or threshold used to measure proliferation) *miR-25*, *miR-106b*, *miR-130b*, *miR1274a*, and *miRPlus-1030*. On the other hand, *miR-29c* is negatively correlated with proliferation and also strongly correlates with estrogen receptor. Estrogen receptor-negative tumors have very low concentrations of microRNAs that are located at 1q, such as *miR-190b*.[18] Another interesting observation is the presence of several microRNAs (*miR532-5p*, *miR-500*, *miR362-5p*, and *miR502-3p*) located at Xp11.23 in cancers with a triple-negative signature and the upregulation of several *miR-17* cluster members in estrogen receptor-negative tumors.

As proliferation is age dependent,[19] we repeated all the analyses for patients aged <71 years ($n=70$ patients). Again, highest overall classification values were found for estrogen receptor, triple-negative and cytokeratin 5 and 6, with 91, 85, and 84% accuracy, respectively, and the analysis of variance *P*-values were highest for estrogen receptor (0.000001) and cytokeratin 5 and 6 (0.00001) (Figure 2). Also in unsupervised hierarchical clustering, the basal-like/triple-negative group is the most easily recognizable. Even though the group of patients under 71 years of age is smaller than the patient group as a whole, the signatures correlating to estrogen receptor/triple-negative/cytokeratin 5 and 6-positive and proliferation are still very stable and highly significant. *MiR-106b* is prominently present in all of these signatures and correlates strongest with high proliferation.

Table 1 Overview for all clinicopathologic features

Variable	N *(%)*	N *(%)*	N *(%)*	*Missing* N *(%)*	*Total*
Nottingham grade 1–2–3	16 (16)	57 (55)	30 (29)		103
Tumor size <2 cm>	61 (59)	41 (40)		1 (1)	103
Mitotic activity index 2	37 (36)	66 (64)			103
Mitotic activity index 3–9	37 (36)	28 (27)	38 (37)		103
Mitotic activity index 10	65 (63)	38 (37)			103
Phosphohistone H3-13	51 (50)	52 (50)			103
Estrogen receptor pos *vs* neg	84 (82)	19 (18)			103
Progesterone receptor pos *vs* neg	87 (84)	15 (15)		1 (1)	103
Her2 neg *vs* pos	83 (81)	19 (18)		1 (1)	103
Triplenegative pos *vs* neg	98 (95)	5 (5)			103
Cytokeratin 5 and 6 neg *vs* pos	87 (84)	14 (14)		2 (2)	103

Discussion

Most microRNA profiling studies have been performed in mixed groups with both lymph node negative and positive breast cancer patients, which are inevitably very heterogeneous. The results of such studies, therefore, must be interpreted with great care. The current study is one of the largest microRNA array studies published regarding lymph node negative breast cancer and also compares microRNA with several important biological features, such as estrogen receptor/progesterone recpetor/Her2/cytokeratin 5 and 6, and proliferation to

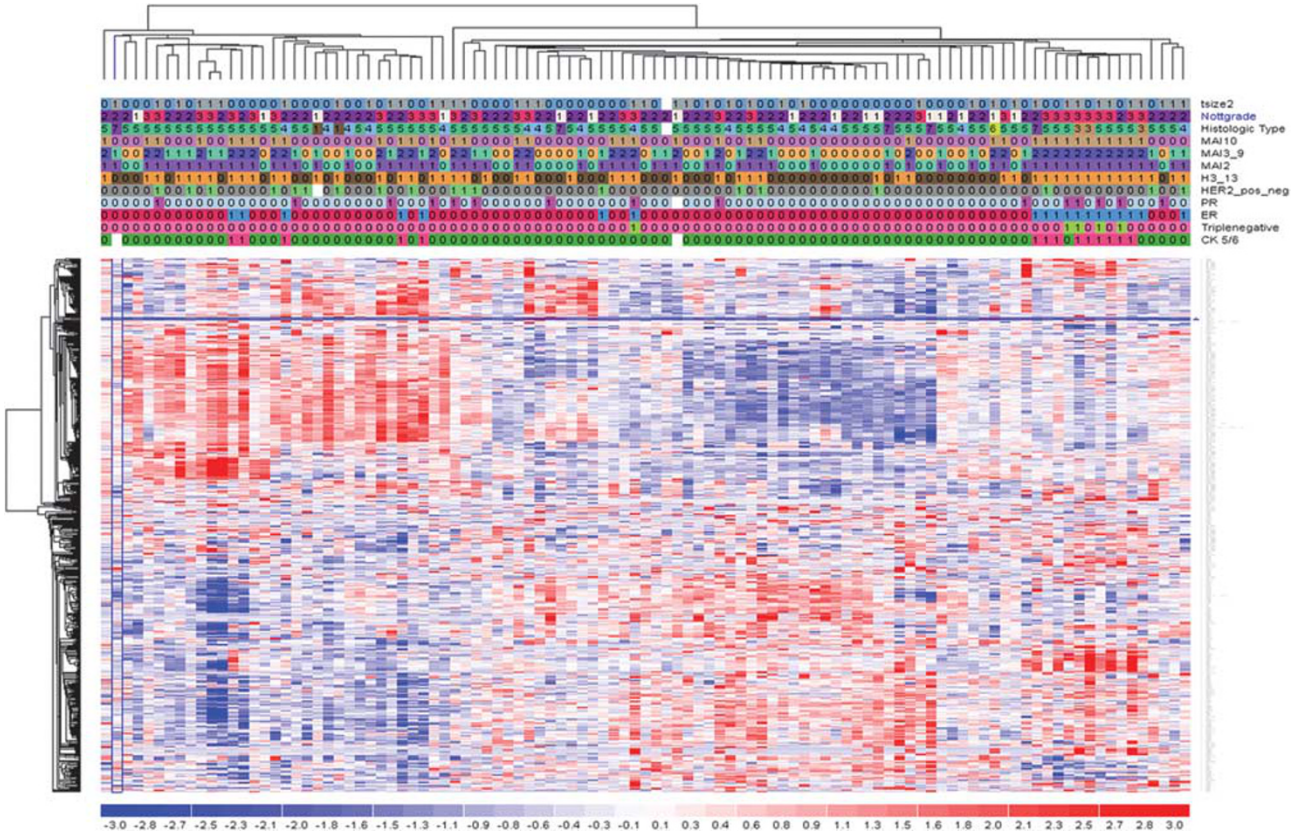

Figure 1 Unsupervised hierarchical clustering for 103 samples and 603 valid microRNAs. The heat map diagram shows the result of the two-way hierarchical clustering of microRNAs and samples. Each row represents a microRNA and each column represents a sample. The microRNA clustering tree is shown on the left, and the sample clustering tree appears at the top. The color scale shown at the bottom illustrates the relative expression level of a microRNA across all samples: red represents an expression level above mean, and blue represents expression lower than the mean. Gray color means that the specific microRNA on a given slide has a signal below background. Numbers for clinicopathological features indicate the following: Tsize2 (Tumor size: $0 \leq 2$ cm, $1 > 2$ cm), Nottgrade (Nottingham grade: 1 = grade 1, 2 = grade 2, 3 = grade 3), histologic type (1 = tubular, 2 = colloid, 3 = medullary, 4 = lobular, 5 = ductal, 6 = mix ductal/lobular), MAI10 (mitotic activity index with threshold 10: $0 < 10$, $1 \geq 10$), MAI3_9 (mitotic activity index with thresholds 3 and 9: $0 < 3$, $1 = \geq 3 - \leq 9$, $2 > 9$), MAI2 (mitotic activity index with threshold 2: ($0 < 3$, $1 \geq 3$), H3_13 (phosphohistone H3 with threshold 13: $0 < 13$, $1 \geq 13$), Her2pos_neg (Her2: 0 = 0 or 1+, 1 = 2+ or 3+), PR (progesterone receptor: $0 \leq 10\%$ positive tumor cells, $1 > 10\%$ positive tumor cells), ER (estrogen receptor) (estrogen receptor: $0 \leq 10\%$ positive tumor cells, $1 > 10\%$ positive tumor cells), Triple-negative (0 = positive for either ER/PR/Her2, 1 = negative for ER and PR and Her2), cytokeratin 5 and 6 (cytokeratin 5 and 6: 0 = no staining, 1 = any percentage of positive tumor cells).

Table 2 Classification results for each clinicopathological feature

Variable	*Classes*	*Strength*	*Number of miR's*	*Prediction rate*	*Overall accuracy*	*Sensitivity*	*Specificity*	*PPV*	*NPV*
Nottingham grade	3	0.0001	12	0.72	46.6	0	97.96	0	76.19
Tumor size	2	0.01	6	0.7	56.73	78.69	26.83	61.54	45.83
MAI2	2	0.0001	21	0.83	68.93	51.35	78.79	57.58	74.29
MAI3-9	3	0.001	59	0.89	42.72	67.74	23.81	56.76	33.33
MAI10	2	0.00001	14	0.83	69.9	84.62	44.74	72.37	62.96
PPH3-13	2	0.0001	19	0.83	66.02	68.63	63.46	64.61	67.35
ER	2	0.0000001	15	0.98	97.09	98.81	89.47	97.65	94.44
PR	2	0.01	26	0.95	79.61	90.80	20.00	86.81	27.27
Her2	2	0.001	5	0.89	78.85	91.57	31.58	85.39	46.15
TNP	2	0.01	41	0.99	90.35	94.95	0	94.95	0
CK5 and 6	2	0.00000001	16	0.97	89.52	96.55	71.43	95.45	76.92

MAI2 (mitotic activity index with threshold 2: ($0 < 3$, $1 \geq 3$), MAI3-9 (mitotic activity index with thresholds 3 and 9: $0 < 3$, $1 = \geq 3 - \leq 9$, $2 > 9$), MAI10 (mitotic activity index with threshold 10: $0 < 10$, $1 \geq 10$), PPH3-13 phosphohistone H3 with threshold 13: $0 < 13$, $1 \geq 13$), ER (estrogen receptor: $0 \leq 10\%$ positive tumor cells, $1 > 10\%$ positive tumor cells), PR (progesterone receptor: $0 \leq 10\%$ positive tumor cells, $1 > 10\%$ positive tumor cells), Her2 (Her2: 0 = 0 or 1+, 1 = 2+ or 3+), TNP (0 = positive for either ER/PR/Her2, 1 = negative for ER and PR and Her2), CK5 and 6 (cytokeratin 5 and 6: 0 = no staining, 1 = any percentage of positive tumor cells).

Table 3 List of all microRNA's correlating with the different clinicopathological features (only those giving the highest classification value are shown).

Nottingham grade	*Tumor size*	*MAI2*	*MAI3-9*	*MAI10*	*PPH3-13*	*ER*	*PR*	*Her2*	*Triple-negative*	*CK5* and *6*
hsa-let-7b	hsa-let-7d*	hsa-let-7b	hsa-let-7a*	hsa-miR-106b	hsa-miR-106b*	hsa-miR-106b	hsa-miR-105	hsa-miR-1285	hsa-let-7b	hsa-miR-106a
hsa-let-7c	hsa-miR-10a	hsa-let-7c	hsa-let-7b	hsa-miR-106b*	hsa-miR-1274a	hsa-miR-106b*	hsa-miR-1265	hsa-miR-1308	hsa-miR-106b	hsa-miR-106b
hsa-miR-106b	hsa-miR-125b-2*	hsa-miR-101	hsa-let-7b*	hsa-miR-1274a	hsa-miR-1280	hsa-miR-135b	hsa-miR-1274a	hsa-miR-135a	hsa-miR-106b*	hsa-miR-135b
hsa-miR-106b*	hsa-miR-126	hsa-miR-1280	hsa-let-7c	hsa-miR-130b	hsa-miR-130b	hsa-miR-181a-2*	hsa-miR-1280	hsa-miRPlus-E1038	hsa-miR-1291	hsa-miR-17
hsa-miR-190b	hsa-miR-210	hsa-miR-1308	hsa-miR-101	hsa-miR-18a	hsa-miR-1826	hsa-miR-18a	hsa-miR-1308	hsa-miRPlus-E1233	hsa-miR-138-1*	hsa-miR-17*
hsa-miR-25*	hsa-miRPlus-F1023	hsa-miR-130b	hsa-miR-106a	hsa-miR-18b	hsa-miR-25*	hsa-miR-18b	hsa-miR-130b		hsa-miR-142-3p	hsa-miR-18a
hsa-miR-29c*		hsa-miR-25*	hsa-miR-106b	hsa-miR-25*	hsa-miR-26a	hsa-miR-190b	hsa-miR-21		hsa-miR-142-5p	hsa-miR-18b
hsa-miR-551b		hsa-miR-26a	hsa-miR-106b*	hsa-miR-29c	hsa-miR-29c	hsa-miR-29c	hsa-miR-21*		hsa-miR-146a	hsa-miR-190b
hsa-miR-584		hsa-miR-584	hsa-miR-10b	hsa-miR-29c*	hsa-miR-29c*	hsa-miR-29c*	hsa-miR-340		hsa-miR-146b-5p	hsa-miR-19a
hsa-miRPlus-E1030		hsa-miR-720	hsa-miR-1274a	hsa-miR-500	hsa-miR-340	hsa-miR-342-3p	hsa-miR-492		hsa-miR-148a	hsa-miR-29c
hsa-miRPlus-E1246		hsa-miRPlus-E1013	hsa-miR-1280	hsa-miR-505	hsa-miR-720	hsa-miR-342-5p	hsa-miR-500*		hsa-miR-155	hsa-miR-29c*
hsa-miRPlus-E1271		hsa-miRPlus-E1024	hsa-miR-1285	hsa-miR-584	hsa-miRPlus-E1013	hsa-miR-378	hsa-miR-519e*		hsa-miR-15b	hsa-miR-342-3p
		hsa-miRPlus-E1030	hsa-miR-1308	hsa-miR-93	hsa-miRPlus-E1030	hsa-miR-505	hsa-miR-629*		hsa-miR-181a-2*	hsa-miR-342-5p
		hsa-miRPlus-E1038	hsa-miR-130b	hsa-miRPlus-E1030	hsa-miRPlus-E1103	hsa-miR-93	hsa-miR-720		hsa-miR-1826	hsa-miR-375
		hsa-miRPlus-E1103	hsa-miR-17		hsa-miRPlus-E1246	hsa-miRPlus-E1219	hsa-miR-890		hsa-miR-203	hsa-miR-505
		hsa-miRPlus-E1114	hsa-miR-17*		hsa-miRPlus-E1271		hsa-miRPlus-E1013		hsa-miR-224	hsa-miRPlus-E1219
		hsa-miRPlus-E1205	hsa-miR-1826		hsa-miRPlus-F1003		hsa-miRPlus-E1024		hsa-miR-25	
		hsa-miRPlus-E1246	hsa-miR-18a		hsa-miRPlus-F1017		hsa-miRPlus-E1038		hsa-miR-32	
		hsa-miRPlus-E1253	hsa-miR-18b		hsa-miRPlus-F1231		hsa-miRPlus-E1103		hsa-miR-362-3p	
		hsa-miRPlus-E1271	hsa-miR-190b				hsa-miRPlus-E1114		hsa-miR-362-5p	
		hsa-miRPlus-F1003	hsa-miR-19a				hsa-miRPlus-E1170		hsa-miR-378	
			hsa-miR-19b				hsa-miRPlus-E1205		hsa-miR-452	
			hsa-miR-224				hsa-miRPlus-E1233		hsa-miR-455-3p	
			hsa-miR-25				hsa-miRPlus-E1253		hsa-miR-455-5p	
			hsa-miR-25*				hsa-miRPlus-E1258		hsa-miR-500	
			hsa-miR-26a				hsa-miRPlus-F1003		hsa-miR-500*	
			hsa-miR-26b						hsa-miR-502-3p	
			hsa-miR-29c						hsa-miR-519d	
			hsa-miR-29c*						hsa-miR-532-3p	
			hsa-miR-30a*						hsa-miR-532-5p	
			hsa-miR-340						hsa-miR-551b	

Table 3 Continued

Nottingham grade	*Tumor size*	*MAI2*	*MAI3-9*	*MAI10*	*PPH3-13*	*ER*	*PR*	*Her2*	*Triple-negative*	*CK5* and *6*
			hsa-miR-342-3p hsa-miR-342-5p hsa-miR-362-5p hsa-miR-375 hsa-miR-381 hsa-miR-492 hsa-miR-500 hsa-miR-505 hsa-miR-584 hsa-miR-663 hsa-miR-720 hsa-miR-874 hsa-miR-93 hsa-miRPlus-B1114 hsa-miRPlus-E1013 hsa-miRPlus-E1024 hsa-miRPlus-E1030 hsa-miRPlus-E1038 hsa-miRPlus-E1103 hsa-miRPlus-E1114 hsa-miRPlus-E1205 hsa-miRPlus-E1218 hsa-miRPlus-E1246 hsa-miRPlus-E1253 hsa-miRPlus-E1258 hsa-miRPlus-E1271 hsa-miRPlus-F1003 hsa-miRPlus-F1017						hsa-miR-576-5p hsa-miR-584 hsa-miR-635 hsa-miR-660 hsa-miR-888* hsa-miR-93 hsa-miRPlus-A1065 hsa-miRPlus-E1170 hsa-miRPlus-E1194 hsa-miRPlus-F1003	

MAI2 (mitotic activity index with threshold 2: ($0<3$, $1\geq3$), MAI3-9 (mitotic activity index with thresholds 3 and 9: $0<3$, $1=\geq3-\leq9$, $2>9$), MAI10 (mitotic activity index with threshold 10: $0<10$, $1\geq10$), PPH3-13 (phosphohistone H3 with threshold 13: $0<13$, $1\geq13$), ER (estrogen receptor: $0\leq10\%$ positive tumor cells, $1>10\%$ positive tumor cells), PR (progesterone receptor: $0\leq10\%$ positive tumor cells, $1>10\%$ positive tumor cells), Her2 (Her2: $0=0$ or 1+, $1=2+$ or 3+), Triple-negative ($0=$positive for either ER/PR/Her2, $1=$negative for ER, PR and Her2), CK5 and 6 (cytokeratin 5 and 6: $0=$no staining, $1=$any percentage of positive tumor cells).

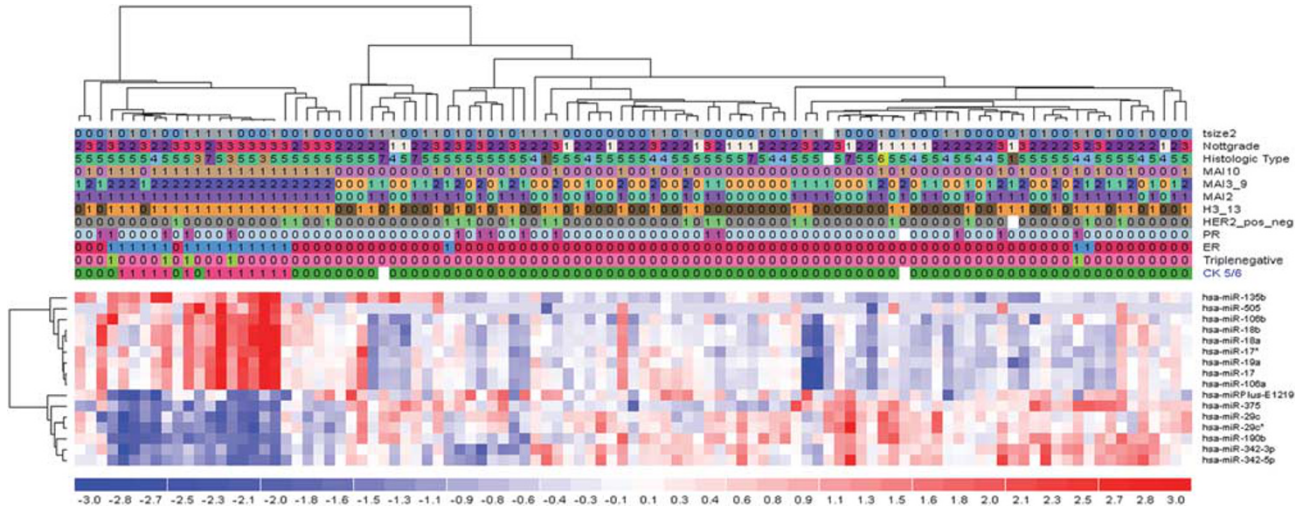

Figure 2 Supervised hierarchical clustering for cytokeratin 5 and 6. The heat map diagram shows the result of the two-way hierarchical clustering of microRNAs and samples. Each row represents a miRNA and each column represents a sample. The microRNA clustering tree is shown on the left, and the sample clustering tree appears at the top. The color scale shown at the bottom illustrates the relative expression level of a microRNA across all samples: red represents an expression level above mean, blue represents expression lower than the mean. Gray color means that the specific microRNA on a given slide has a signal below background. Numbers for clinicopathological features indicate the following: Tsize2 (Tumor size: $0 \leq 2$ cm, $1 > 2$ cm), Nottgrade (Nottingham grade: 1 = grade 1, 2 = grade 2, 3 = grade 3), histologic type (1 = tubular, 2 = colloid, 3 = medullary, 4 = lobular, 5 = ductal, 6 = mix ductal/lobular), MAI10 (mitotic activity index with threshold 10: $0 < 10$, $1 \geq 10$), MAI3_9 (mitotic activity index with thresholds 3 and 9: $0 < 3$, $1 = \geq 3 - \leq 9$, $2 > 9$), MAI2 (mitotic activity index with threshold 2: $(0 < 3$, $1 \geq 3)$, H3_13 (phosphohistone H3 with threshold 13: $0 < 13$, $1 \geq 13)$, Her2pos_neg (Her2: 0 = 0 or 1+, 1 = 2+ or 3+), PR (progesterone receptor: $0 \leq 10\%$ positive tumor cells, $1 > 10\%$ positive tumor cells), ER (estrogen receptor: $0 \leq 10\%$ positive tumor cells, $1 > 10\%$ positive tumor cells), Triple-negative (0 = positive for either ER/PR/Her2, 1 = negative for ER and PR and Her2), cytokeratin 5 and 6 (cytokeratin 5 and 6: 0 = no staining, 1 = any percentage of positive tumor cells).

create more insight into their fundamental regulation. We found that estrogen receptor negativity and cytokeratin 5 and 6 positivity are the most prominent biological features with unique microRNA profiles. Furthermore, several microRNAs were found that correlate with high proliferation, which is important as proliferation is the strongest single prognosticator in this group of lymph node negative patients.[14] Being able to modulate the level of microRNAs involved in proliferation, such as mir-106B, might, therefore, offer new possibilities for treating patients.

Although most of the microRNA studies have been performed using mixed groups of both lymph node negative and -positive breast cancer patients with earlier versions of arrays (thereby, including fewer microRNAs), several microRNAs have been described before in relation to estrogen receptor/progesterone receptor/triple-negative/cytokeratin 5 and 6 and proliferation. miR-342 was found to be higher in luminal B subtype breast cancer and lowest in the triple-negative/basal-like subtype,[20] and furthermore, miR-342 level as measured by quantitative reverse transcriptase-PCR was found to positively correlate with Her2 positivity. In our study, miR-342 was especially low in estrogen receptor-negative tumors and cytokeratin 5 and 6 positive tumors. Although miR-342 has also been found to be downregulated in tamoxifen- resistant breast cancer cells compared with tamoxifen-sensitive cells,[21] a clear target with a link to the triple-negative/basal-subtype and tamoxifen resistance has not been described as yet.

In vitro experiments have shown that miR-18a can directly bind to the 3′-untranslated region of estrogen receptor-α, both overexpression of the precursor pre-miR-18a, and mature miR-18a could result in a considerable reduction of estrogen receptor protein.[22] Adding estradiol to estrogen receptor-α-positive cell lines resulted in immediate upregulation of pri-mir17-92 expression, most likely by recruiting c-MYC to the mir-17-92 promoter. Furthermore, in women with a hepatocellular carcinoma, miR-18a expression correlated with reduced estrogen receptor-α and caused increased proliferation,[23] thereby supporting our findings that miR18a is highly expressed in high-proliferating estrogen receptor-α negative tumors. MiR-106b, also found to be upregulated in high-proliferating estrogen receptor-α negative tumors, has been described to be able to negatively regulate AIB1 protein translation by a direct interaction with the 3′-untranslated region of AIB1 mRNA, and is also able to downregulate p21.[24] Transfection with mir-106b could even prevent p53-induced blockage of the cell cycle at the G1-S checkpoint, after doxorubicin-induced DNA-damage, probably by silencing p21.[25] Other members of the mir-106b family, eg miR-93 and miR-106a, are also positively correlated with proliferation; transfection of mir-106a resulted in an increase by 14–15% in the number of S-phase cells.[25] Both mir-93 and mir-130b have been

described to target the 3′ untranslated region of the mRNA for a tumor suppressor protein, tumor protein 53-induced nuclear protein 1.[26] Overexpression of tumor protein 53-induced nuclear protein 1 induces cell-cycle arrest and apoptosis in several cell lines, even in the absence of p53. In this case, tumor protein 53-induced nuclear protein 1 is functionally associated with p73 and allows regulation of cell-cycle progression and apoptosis, independent of p53.[27]

In agreement with Lowery *et al*,[20] mir135b was also inversely correlated with estrogen receptor in our study: one possible target for mir-135b is the estrogen-related receptor α according to PicTar. This protein is an orphan member of the superfamily of hormone nuclear receptors, and has been shown to have a key role in the regulation of estrogen-responsive genes by efficiently binding estrogen-responsive elements leading either to modulation of the response to estrogens or functional substitution for estrogen receptor as a constitutive activator of estrogen responsive elements-dependent transcription. In estrogen receptor-negative cell lines, estrogen-related receptor-α has been shown to act as an constitutive, estrogen-independent activator of transcription of estrogen responsive elements-dependent transcription.[28] One of the target genes for such activation is Osteopontin, a secreted protein that is over-expressed in a number of human cancers, and has been associated with increased metastatic burden and poor prognosis in breast cancer patients.[29] Other microRNAs that inversely correlate with estrogen receptor-α expression are mir-505 and mir-181a-2*, and although little is known about these miRs, mir-181a has been described to target p27 in myeloid leukemia cells.[30]

MiR-29c is downregulated in estrogen receptor-α negative, cytokeratin 5 and 6 positive and high proliferating tumors, and has recently been described to upregulate p53 and directly suppress p85α (the regulatory subunit of PI3 kinase) and CDC42 (a Rho family guanosine triphosphatase), both of which negatively regulate p53.[31]

The current study shows that estrogen receptor negativity and cytokeratin 5 and 6 expression are important biological processes in lymph node negative breast cancer as the correlations with specific microRNAs are strongest in the estrogen receptor negative and cytokeratin 5 and 6 positive tumors. Although proliferation is a strong prognosticator in lymph node negative breast cancer, it is clearly the end product of different biological processes, thereby making it more difficult to separate the low from the high proliferative group. As mRNA profiling studies have shown, larger numbers of tumors need to be analyzed to confirm these results and each individual microRNA needs to be investigated more thoroughly in both formaldehyde-fixed paraffin embedded tissues and in cell cultures, for localization and biological function.

Acknowledgements

The authors are grateful for the grant provided by the Folke Hermansen Fond in 2007, and a grant provided by the Stavanger University Hospital research fund in 2009. Kristin Jonsdottir is supported by a grant from Helse Vest. Dr H Pinheiro and Dr C Glue from Exiqon are thanked for their excellent help in setting up the study and analyzing the data.

Disclosure/conflict of interest

The authors declare no conflict of interest.

References

1 Perou CM, Sorlie T, Eisen MB, *et al.* Molecular portraits of human breast tumours. Nature 2000;406: 747–752.
2 Cheang MC, Voduc D, Bajdik C, *et al.* Basal-like breast cancer defined by five biomarkers has superior prognostic value than triple-negative phenotype. Clin Cancer Res 2008;14:1368–1376.
3 Rakha EA, El-Sayed ME, Lee AH, *et al.* Prognostic significance of Nottingham histologic grade in invasive breast carcinoma. J Clin Oncol 2008;26:3153–3158.
4 Git A, Spiteri I, Blenkiron C, *et al.* PMC42, a breast progenitor cancer cell line, has normal-like mRNA and microRNA transcriptomes. Breast Cancer Res 2008;10:R54.
5 Desmedt C, Haibe-Kains B, Wirapati P, *et al.* Biological processes associated with breast cancer clinical outcome depend on the molecular subtypes. Clin Cancer Res 2008;14:5158–5165.
6 Baak JP, Gudlaugsson E, Skaland I, *et al.* Proliferation is the strongest prognosticator in node-negative breast cancer: significance, error sources, alternatives and comparison with molecular prognostic markers. Breast Cancer Res Treat 2009;115:241–254.
7 Baak JP, Kruse AJ, Robboy SJ, *et al.* Dynamic behavioural interpretation of cervical intraepithelial neoplasia with molecular biomarkers. J Clin Pathol 2006;59:1017–1028.
8 Andre F, Khalil A, Slimane K, *et al.* Mitotic index and benefit of adjuvant anthracycline-based chemotherapy in patients with early breast cancer. J Clin Oncol 2005;23:2996–3000.
9 Bartel DP. MicroRNAs: genomics, biogenesis, mechanism, and function. Cell 2004;116:281–297.
10 Mothe BR, Stewart BS, Oseroff C, *et al.* Chronic lymphocytic choriomeningitis virus infection actively down-regulates CD4+ T cell responses directed against a broad range of epitopes. J Immunol 2007;179:1058–1067.
11 Welch C, Chen Y, Stallings RL. MicroRNA-34a functions as a potential tumor suppressor by inducing apoptosis in neuroblastoma cells. Oncogene 2007;26:5017–5022.
12 Tavassoli FA, Devilee P, (eds) World Health Organization Classification of Tumors Pathology and Genetics of Tumors of the Breast and Female and Genital Organs. IARC Press: Lyon, 2003.
13 Elston CW, Ellis IO. Pathological prognostic factors in breast cancer. I. The value of histological grade in

breast cancer: experience from a large study with long-term follow-up. Histopathology 1991;19:403–410.
14 Baak JP, van Diest PJ, Voorhorst FJ, *et al.* Prospective multicenter validation of the independent prognostic value of the mitotic activity index in lymph node-negative breast cancer patients younger than 55 years. J Clin Oncol 2005;23:5993–6001.
15 Skaland I, Janssen EA, Gudlaugsson E, *et al.* Phosphohistone H3 expression has much stronger prognostic value than classical prognosticators in invasive lymph node-negative breast cancer patients less than 55 years of age. Mod Pathol 2007;20:1307–1315.
16 Bossard C, Jarry A, Colombeix C, *et al.* Phosphohistone H3 labelling for histoprognostic grading of breast adenocarcinomas and computer-assisted determination of mitotic index. J Clin Pathol 2006;59:706–710.
17 Boenisch T. Formalin-fixed and heat-retrieved tissue antigens: a comparison of their immunoreactivity in experimental antibody diluents. Appl Immunohistochem Mol Morphol 2001;9:176–179.
18 Natrajan R, Lambros MB, Rodriguez-Pinilla SM, *et al.* Tiling path genomic profiling of grade 3 invasive ductal breast cancers. Clin Cancer Res 2009;15:2711–2722.
19 Baak JP, van Diest PJ, Voorhorst FJ, *et al.* The prognostic value of proliferation in lymph-node-negative breast cancer patients is age dependent. Eur J Cancer 2007;43:527–535.
20 Lowery AJ, Miller N, Devaney A, *et al.* MicroRNA signatures predict estrogen receptor, progesterone receptor and HER2/neu receptor status in breast cancer. Breast Cancer Res 2009;11:R27.
21 Davoren PA, McNeill RE, Lowery AJ, *et al.* Identification of suitable endogenous control genes for microRNA gene expression analysis in human breast cancer. BMC Mol Biol 2008;9:76.
22 Castellano L, Giamas G, Jacob J, *et al.* The estrogen receptor-alpha-induced microRNA signature regulates itself and its transcriptional response. Proc Natl Acad Sci USA 2009;106:15732–15737.
23 Chen GQ, Zhao ZW, Zhou HY, *et al.* Systematic analysis of microRNA involved in resistance of the MCF-7 human breast cancer cell to doxorubicin. Med Oncol 2010;27:406–415.
24 Petrocca F, Visone R, Onelli MR, *et al.* E2F1-regulated microRNAs impair TGFbeta-dependent cell-cycle arrest and apoptosis in gastric cancer. Cancer Cell 2008;13:272–286.
25 Ivanovska I, Ball AS, Diaz RL, *et al.* MicroRNAs in the miR-106b family regulate p21/CDKN1A and promote cell cycle progression. Mol Cell Biol 2008;28:2167–2174.
26 Yeung ML, Yasunaga J, Bennasser Y, *et al.* Roles for microRNAs, miR-93 and miR-130b, and tumor protein 53-induced nuclear protein 1 tumor suppressor in cell growth dysregulation by human T-cell lymphotrophic virus 1. Cancer Res 2008;68:8976–8985.
27 Tomasini R, Seux M, Nowak J, *et al.* TP53INP1 is a novel p73 target gene that induces cell cycle arrest and cell death by modulating p73 transcriptional activity. Oncogene 2005;24:8093–8104.
28 Kraus RJ, Ariazi EA, Farrell ML, *et al.* Estrogen-related receptor alpha 1 actively antagonizes estrogen receptor-regulated transcription in MCF-7 mammary cells. J Biol Chem 2002;277:24826–24834.
29 Tuck AB, O'Malley FP, Singhal H, *et al.* Osteopontin expression in a group of lymph node negative breast cancer patients. Int J Cancer 1998;79:502–508.
30 Wang X, Gocek E, Liu CG, *et al.* MicroRNAs181 regulate the expression of p27Kip1 in human myeloid leukemia cells induced to differentiate by 1,25-dihydroxyvitamin D3. Cell Cycle 2009;8:736–741.
31 Park SY, Lee JH, Ha M, *et al.* miR-29 miRNAs activate p53 by targeting p85 alpha and CDC42. Nat Struct Mol Biol 2009;16:23–29.